MONITORING TWO BEAMS IN AHF BEAM SPLITTERS

S.S. Kurennoy, Los Alamos National Laboratory, Los Alamos, NM 87545, USA

Abstract

The beam transport system for the Advanced Hydrotest Facility (AHF) anticipates multiple beam splitters. Monitoring two transversely separated beams in a common beam pipe in the splitter sections imposes certain requirements on beam diagnostics for these sections. We explore a two-beam system in a generic beam monitor and study the feasibility of resolving the transverse positions of the two beams with one diagnostics device. Effects of unequal currents in two beams and of finite transverse beam sizes are explored analytically for both the ultra relativistic case and in the long-wavelength limit.

1 INTRODUCTION

In the planned Advanced Hydrotest Facility (AHF) [1], 20-ns beam pulses (bunches) will be extracted from the 50-GeV main proton synchrotron and then transported to the target by an elaborated transport system. The beam transport system splits the beam bunches into two parts (beamlets) in its splitting sections, either with equal currents or in the ratio 2:1, so that up to 12 synchronous beam pulses of equal intensity can be delivered to the target for multi-axis proton radiography. Information about the transverse positions of the beams in the splitters should be delivered by some diagnostic devices. Possible candidates are wall current monitors or conventional stripline beam position monitors (BPMs). We need estimates on how well the transverse positions of the two beams can be resolved by these monitors.

2 FIELDS AND BPM SIGNALS

Let us make the following assumptions: (i) the vacuum chamber near the monitors is homogeneous along the chamber axis; (ii) its walls are perfectly conducting, and (iii) $(\omega b/\beta\gamma c)^2 \ll 1$, where ω is the frequency of interest and b is a typical transverse dimension of the chamber. Condition (iii) includes both the ultra relativistic limit and the long-wavelength limit, when the wavelength $\lambda \gg b$. For the AHF with 50-GeV protons and with b on the order of 10 cm, the condition (iii) is satisfied up to 10 GHz. The calculation of the beam transverse field on the chamber walls is then a 2-D electrostatic problem. This field can be treated as a sum of fields produced by thin (pencil) beams plus corrections due to finite transverse beam sizes. An arbitrary transverse distribution of the beam current in a chamber of a general cross section was studied in Ref. [2], where beam-size corrections to the BPM signals were calculated. In our case, the current distribution is just a sum of distributions of two separate beams, see Fig. 1. From the transverse electric field created by two beams at an arbitrary point on the chamber wall we find the induced wall currents, and hence, the BPM signals.

An input beam in the AHF splitter sections is split in the horizontal plane initially by an electrostatic septum, and then two beamlets are further separated by one pulsed and two DC magnetic septa [1]. Separated beamlets in a splitter are illustrated in Fig. 1; the beam pipe has a circular cross section.

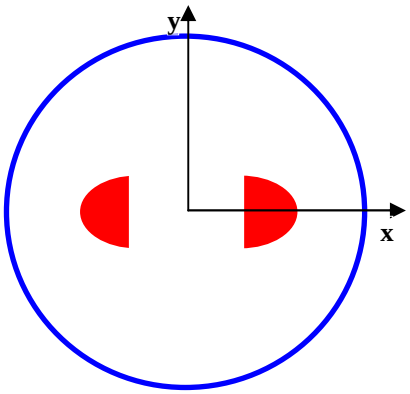

Figure 1: Transverse cross section of the vacuum chamber (blue) and of two split beams (red) in AHF beam splitters.

Let us assume that the centers of the charge transverse distributions $\lambda_i(x,y)$ in two beams, i=1,2, are located at $\vec{r}_i$, and their currents have the ratio of k to (1-k), so that k=1/2 corresponds to two equal beams, each with unit charge per unit length. The transverse field created at a point $\vec{b}$ on the wall of a circular pipe of radius b by a pencil beam with its axis displaced from the chamber axis by $\vec{r}$ (or, equivalently, by an axisymmetric distribution of charge having the same axis, see in [2]) is well-known:

$$e(\vec{r},\vec{b}) = \frac{1}{2\pi b}\,\frac{b^2 - r^2}{b^2 - 2\vec{b}\vec{r} + r^2}. \qquad (1)$$

Due to linearity, for two pencil beams the resulting field is

$$E(\vec{r}_1,\vec{r}_2,\vec{b}) = 2ke(\vec{r}_1,\vec{b}) + 2(1-k)e(\vec{r}_2,\vec{b}). \qquad (2)$$

Introducing the center of the two-beam charge distribution $\vec{a} = k\vec{r}_1 + (1-k)\vec{r}_2$, and the beam spacing $\vec{d} = \vec{r}_1 - \vec{r}_2$, we can rewrite Eqs. (1-2) in terms of $\vec{a},\vec{d}$. Since the induced wall currents are proportional to the field (2), integrating it within the BPM electrode azimuthal range gives us the BPM signal from the two pencil beams. Adding two sets of beam-size corrections as in Ref. [2] (one for each of two beams) produces the required results for BPM signals due to two beams. For practical purposes it is useful to derive simple expressions for BPM signals as functions of the beam positions and sizes. For simplicity, let us consider a stripline BPM with four narrow electrodes in the points **R** (b,0), **T** (0,b), **L** (-b,0), and **B** (0,-b) of Fig. 1. Accounting for a finite width of electrodes would lead to additional formfactors in equations for BPM signals, cf. in [2]; these formfactors tend to 1 for narrow electrodes.

2.1 BPM Signal Ratios: Small Beam Offsets

If we choose $b=1$, so that all transverse dimensions are in units of *b*, for the case of small beam displacements from the chamber axis – $|a_x|,|a_y|,|d_x|,|d_y| \ll 1$ – one can expand the BPM signal ratios as follows:

$$\begin{aligned} H &\equiv \frac{R-L}{S} = a_x + a_x\left[a_x^2 - 3a_y^2 + 3k(1-k)\left(d_x^2 - d_y^2\right)\right] - \\ &\quad 6k(1-k)a_y d_x d_y + k(1-k)(1-2k)d_x\left(d_x^2 - 3d_y^2\right); \\ V &\equiv \frac{T-B}{S} = a_y + a_y\left[a_y^2 - 3a_x^2 - 3k(1-k)\left(d_x^2 - d_y^2\right)\right] - \\ &\quad 6k(1-k)a_x d_x d_y + k(1-k)(1-2k)d_y\left(d_y^2 - 3d_x^2\right); \\ Q &\equiv \frac{(R+L)-(T+B)}{S} = 2\left(a_x^2 - a_y^2\right) + 2k(1-k)\left(d_x^2 - d_y^2\right), \end{aligned} \tag{3}$$

where *R,L,T,B* are BPM signals on the corresponding electrodes, $S = R+L+T+B$ is a sum signal, and terms of the order $O(\delta^4)$ are omitted in expansions (3). For thick beams, the beam-size corrections should be added to ratios (3). The lowest order beam-size corrections enter (3) via the combination of beam quadrupole moments M_2: $3a_x M_2$, $-3a_y M_2$, and $2M_2$ should be added to Eqs. (3), correspondingly, where $M_2 \equiv kM_2^{(1)} + (1-k)M_2^{(2)}$, and the beam distribution quadrupole moments are

$$M_2^{(i)} = \int_{S_i} dxdy\lambda_i(x,y)(x^2 - y^2). \tag{4}$$

In Eq. (4), the integration goes along the beam cross section S_i in the beam local coordinates, where (0,0) is the beam center. Definitions of some normalized charge distributions functions and their quadrupole moments are listed in Table 1: {1} is double-Gaussian, {2} is uniform rectangular. For non-symmetric distributions: uniform rhs semicircle {3}, semi-elliptic rhs double-Gaussian {4}, – Δ_x is the distance between the cut edge and the beam center: $\Delta_x = 4\sigma/3\pi$ for {3} and $\Delta_x = \sigma_x\sqrt{2/\pi}$ in {4}.

Table 1: Some transverse distributions of beam charge.

	$\lambda(x,y)$, center at $(x=0, y=0)$	M_2
{1}	$\frac{1}{2\pi\sigma_x\sigma_y}\exp\left[-\frac{x^2}{2\sigma_x^2} - \frac{y^2}{2\sigma_y^2}\right]$	$\sigma_x^2 - \sigma_y^2$
{2}	$\theta(x+\sigma_x)\theta(\sigma_x - x)\times$ $\theta(y+\sigma_y)\theta(\sigma_y - y)/(4\sigma_x\sigma_y)$	$\frac{\sigma_x^2 - \sigma_y^2}{3}$
{3}	$\frac{2}{\pi\sigma^2}\theta\left[\sigma^2 - x^2 - y^2\right]\theta(x+\Delta_x)$	$-\frac{16}{9\pi^2}\sigma^2$
{4}	$\frac{\theta(x+\Delta_x)}{\pi\sigma_x\sigma_y}\exp\left[-\frac{(x+\Delta_x)^2}{2\sigma_x^2} - \frac{y^2}{2\sigma_y^2}\right]$	$\sigma_x^2 - \sigma_y^2$ $-2\sigma_x^2/\pi$

For the case when the horizontal beam separation is larger than other transverse offsets and sizes, i.e. when $|a_x|,|a_y|,|d_y|,|\sigma_i| \ll |d_x| \ll 1$, the quadrupole ratio *Q* in (3) becomes $Q \cong 2k(1-k)d_x^2$. This relation can be used to derive the horizontal beam separation d_x directly from BPM measurements of *Q*, when the value of the charge misbalance *k* is known, either by design or from current measurements downstream of the splitter, where two beams are in separate beam pipes. After k, d_x are known, the position of the two-beam system center (a_x, a_y) can be found from the leading terms in Eqs. (3):

$$\begin{aligned} H &\cong k(1-k)(1-2k)d_x^3 + a_x\left[1 + 3k(1-k)d_x^2\right]; \\ V &\cong a_y\left[1 - 3k(1-k)d_x^2\right]. \end{aligned} \tag{5}$$

2.2 BPM Signal Ratios: Large Beam Separation

When the horizontal beam separation becomes large in the AHF splitters, i.e. $1 \le |d_x| < 2$ (again, in units of the chamber radius *b*), the expressions for BPM signal ratios have to be modified. The leading (zeroth-order) term of the quadrupole ratio (again, $|a_x|,|a_y|,|d_y|,|\sigma_i| \ll 1$) is

$$Q \cong \frac{2k(1-k)d_x^2\left\{1 - k(1-k)\left[1 - 3k(1-k)\right]d_x^4\right\}}{1 - (1-2k)^2\left[1 - 2k(1-k)\right]d_x^4 - k^4(1-k)^4 d_x^8}. \tag{6}$$

Even the first-order terms here are too cumbersome, and therefore omitted; see [3] for more details. For two equal beams, the results look simpler:

$$\begin{aligned} H &\cong a_x\frac{\left(1+h_x^2\right)^2}{\left(1-h_x^2\right)\left(1+h_x^4\right)} - 2a_y h_y\frac{h_x\left(1+h_x^2\right)\left(3+h_x^2\right)}{\left(1-h_x^2\right)^2\left(1+h_x^4\right)}; \\ V &\cong a_y\frac{\left(1-h_x^2\right)^2}{\left(1+h_x^2\right)\left(1+h_x^4\right)} - 2a_x h_y\frac{h_x\left(1-h_x^2\right)\left(3-h_x^2\right)}{\left(1+h_x^2\right)^2\left(1+h_x^4\right)}; \\ Q &\cong 2\frac{h_x^2}{1+h_x^4} + 2\frac{1+3h_x^2}{\left(1+h_x^4\right)^2}\left(a_x^2 - a_y^2 - h_y^2\right), \end{aligned} \tag{7}$$

where notation $\vec{h} \equiv \vec{d}/2$ was introduced for compactness.

One should mention that the beam-size corrections to Eqs. (6,7) are exactly the same as those in (3); they are independent of the beam separation in the lowest order.

3 ESTIMATES FOR AHF SPLITTERS

According to beam dynamics simulations [1,4], two beamlets in the AHF splitter sections look as shown in Fig. 1, and their transverse beam-charge distributions can be approximated by semi-elliptic double-Gaussian ones (cf. distribution {4} in Table 1 for the rhs beam), with the rms values σ_x=3.7 mm and σ_y=2.4 mm. The horizontal beam separation *g*, from one beam cut edge to the other, increases from 5 mm near the entrance to the pulsed magnetic septum to about 5.2 cm at the entrance of the

first DC magnetic septum. The vacuum pipe ID changes from 2" to 4", correspondingly. These two locations are the best ones for a diagnostic device that can be called "quadrupole monitor". The center-to-center horizontal beam separation $d_x = g + 2\Delta_x$, so that the ratio d_x / b is equal to 0.43 and 1.14 at these two points, respectively. The quadrupole ratios for equal currents at the two points are Q_1=0.088 (from Eq. (3); it includes the beam-size correction of -0.003), and Q_2=0.586 from Eq. (7) (here the beam-size correction is -0.0008). Other corrections to Q are below a few percent when $|a_x|, |a_y|, |d_y| < 0.15b$. We should emphasize that the beam-size corrections are rather small in this case.

Expansions (3,5-7) for BPM signal ratios in terms of the beam parameters are simple enough to allow an effective processing of BPM signals to extract data on the beam separation and centering. Since the exact result (2) for the transverse fields is available, we can compare the derived expansions with it. Figures 2-4 show dependences of the quadrupole BPM signal ratio Q on various parameters of the two-beam system.

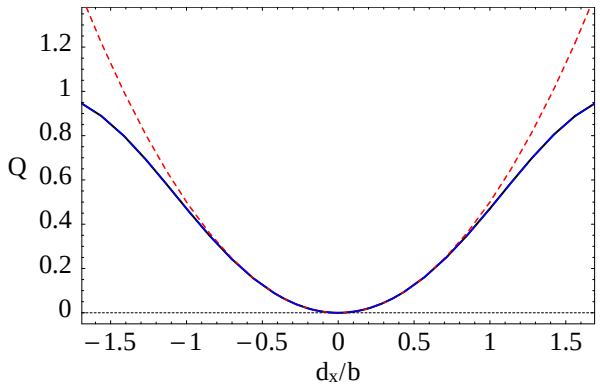

Figure 2: Quadrupole signal ratio versus beam separation for k=0.5, $a_{x,y}$=0, d_y=0: exact Eq. (2) (black solid curve), Eq. (3) (red short-dashed), Eq. (7) (blue dashed).

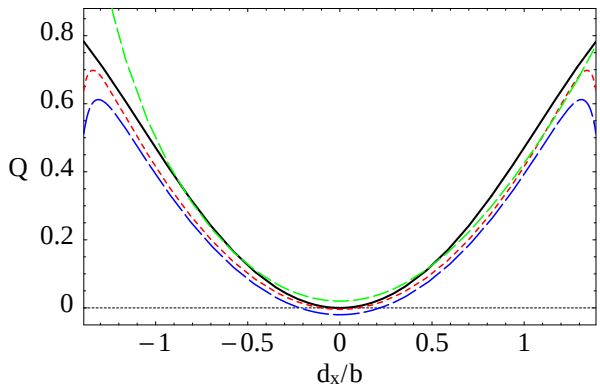

Figure 3: The same, from exact Eq. (2), with: k=0.5, $a_{x,y}$=0, d_y=0 (black solid); k=0.3, $a_{x,y}$=0, d_y=0.1b (red short-dashed); k=0.7, a_x=0.1b, a_y=0, d_y=0 (green dashed); k=0.7, a_x=0, a_y=0.1b, d_y=0 (blue long-dashed).

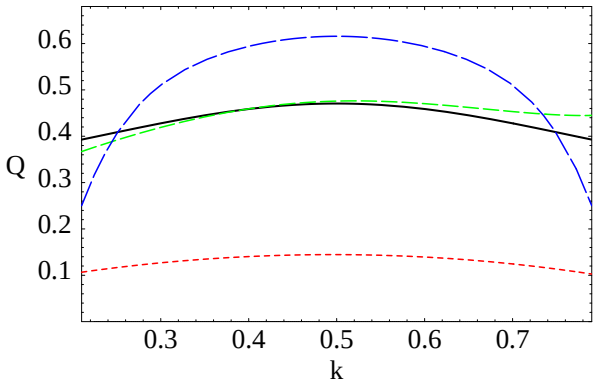

Figure 4: Q ratio versus current misbalance k: $a_{x,y}$=0, d_x=b, d_y=0 (black solid); a_x=0.1b, a_y=0, d_x=0.5b, d_y=0 (red short-dashed); a_x=0, a_y=-0.05b, d_x=b, d_y=0 (green dashed); $a_{x,y}$=0, d_x=1.2b, d_y=0.2b (blue long-dashed).

One can see that the expansions (3,5-7) for BPM signal ratios work quite well in their regions of applicability. Deviations of the two-beam center from the axis do not change Q significantly for the parameters relevant to the AHF splitters, as demonstrated in Fig. 3. Results for H and V ratios, as well as more details, can be found in [3].

4 CONCLUSIONS

The transverse field produced by two separated beams in a vacuum chamber has been calculated as a sum of the fields of two pencil (thin) beams plus corrections due to transverse distributions of currents in two beams. It is shown that for relatively large horizontal beam separations in a circular vacuum chamber, measurements in four points on the chamber walls (e.g., performed with a 4-stripline BPM) allow us to reliably determine the horizontal separation of two beams from the quadrupole ratio of signals, even if two beam currents differ by a factor of 2. If two separated beams have almost equal currents, or alternatively, if their current ratio is known from independent measurements by current monitors, one can also obtain from the BPM measurements the position of the center of the two-beam system.

Estimates for the AHF beam splitters show feasibility of resolving the beam separation and the position of the two-beam center using non-interruptive measurements with a simple 4-stripline BPM.

The author would like to acknowledge useful discussions with B. Blind, J.D. Gilpatrick, and A.J. Jason.

5 REFERENCES

[1] "Advanced Hydrotest Facility FY2000 Trade Study Report", Los Alamos report LA-CP-00-379, 2000.

[2] S.S. Kurennoy, "Nonlinearities and effects of transverse beam size in beam position monitors", Phys. Rev. ST Accel. & Beams, 092801 (2001).

[3] S.S. Kurennoy, "Resolving two beams in beam splitters with a beam position monitor", LA-UR-02-2768, 2002; also physics/0205066 at www.arxiv.org.

[4] B. Blind, private communication.